



Research paper

Stronger ecosystem carbon sequestration potential of mangrove wetlands with respect to terrestrial forests in subtropical China

Xiaowei Cui^{a,b}, Jie Liang^b, Weizhi Lu^{a,c}, Hui Chen^{a,d}, Fang Liu^b, Guangxuan Lin^e, Fanghong Xu^e, Yiqi Luo^b, Guanghui Lin^{a,b,*}^a Division of Ocean Science and Technology, Graduate School at Shenzhen, Tsinghua University, Shenzhen, Guangdong 518055, China^b Ministry of Education Key Laboratory for Earth System Modeling, Department of Earth System Science, Institute for Global Change Research, Beijing 100084, China^c National Marine Environmental Monitoring Center, State Oceanic Administration, Dalian 116023, China^d College of Life Science, Yangtze University, Jingzhou 434025, China^e Bureau for Zhanjiang National Mangrove Nature Reserve, Zhanjiang, Guangdong 524044, China

ARTICLE INFO

Keywords:

Mangrove wetland
Terrestrial forest
Carbon sink
Eddy covariance technique
Subtropical China

ABSTRACT

Mangrove wetlands and terrestrial forests are considered as important carbon sinks for alleviating climate changes, but the sequestration processes and regulations of climate factors on controlling the variability of carbon fluxes of these ecosystems may differ. In order to compare the different mechanisms of carbon sequestration in mangrove and terrestrial forest ecosystems, we analyzed ecosystem CO₂ flux data measured by eddy covariance (EC) technique from four forests ecosystems in subtropical China: two mangrove wetlands and two terrestrial forests. Our results showed that the mangrove wetlands could sequester much more carbon than the nearby terrestrial forests because of significantly higher gross ecosystem production (GEP) and lower ecosystem respiration (Re) values. Moreover, our analysis of the responses of net ecosystem exchange (NEE) to photosynthetically active radiation showed that the mangrove wetlands had lower light compensation point but higher maximum photosynthesis rates than the terrestrial forests. Furthermore, the relationships between Re and air temperature (T_{air}) showed the ecosystem respiration rate (Re_{ref}) at 20 °C values were lower but that the temperature sensitivity (Q₁₀) values were higher in the mangrove wetlands than in the terrestrial forests, which might be caused by tides in the mangrove ecosystems. In addition, the relationships between the logarithmic values of soil organic carbon ln(SOC) and δ¹³C indicated that SOC decomposition rates were lower in mangrove forests than in terrestrial forests, which thus led to lower Re values compared to terrestrial forests. Our results imply that mangrove forests can sequester more CO₂ from the atmosphere than nearby terrestrial forests due to relatively higher GEP and lower Re values. Moreover, the regulation of ecosystem carbon exchange by tides in mangrove wetlands should be investigated in more detail in future studies.

1. Introduction

Continuously increasing CO₂ concentration led to an imbalance in the carbon budget in the Earth's atmosphere affect the climate. Therefore, accurately describing global and regional carbon fluxes and exchange processes is crucial to understanding the mechanism and predicting the trends of future climate change (Feng et al., 2017; Lu et al., 2017; Wilson et al., 2007; Yu et al., 2011). Generally, terrestrial forests are considered to be sinks of atmospheric CO₂ and play a dominant role in mitigating climate changes (Piao et al., 2009; Yu et al., 2013). Mangrove wetlands are woody forests distributed along the coast in tropical and subtropical zones, and they are thought to be one of the most carbon-rich ecosystems in the tropics (Donato et al., 2011).

Mangrove wetlands sequesters approximately 218 Tg C y⁻¹ from the atmosphere and this carbon is a key component of so called “blue carbon” (Artigas et al., 2015; Mcleod et al., 2011). Exploring the differences in the CO₂ flux dynamics between mangrove wetlands and terrestrial forests is essential for understanding the mechanisms of carbon cycle and providing a theoretical basis for modeling carbon pool variations and the CO₂ exchange rates (Polsenaere et al., 2012; Yu et al., 2013).

Eddy covariance (EC) measurements offer a method to continuously measure carbon flux and meteorological data across regions and vegetation cover types, which has been applied to analyze carbon exchange dynamics in terrestrial and mangrove ecosystems at different spatial and temporal scales (Brunner et al., 2012; Coursolle et al., 2006;

* Corresponding author at: Division of Ocean Science and Technology, Graduate School at Shenzhen, Tsinghua University, Shenzhen, Guangdong 518055, China.
E-mail addresses: lin.guanghui@sz.tsinghua.edu.cn, lingh@tsinghua.edu.cn (G. Lin).

Moffat et al., 2007; Baldocchi, 2008; Bouillon et al., 2008; Jung et al., 2011; Lu et al., 2014; Xiao et al., 2011a,b). Previous studies on carbon flux dynamics in terrestrial forests showed that both natural and planted forests were large carbon sinks (Bracho et al., 2012; Lund et al., 2010; Tan et al., 2011; Yi et al., 2010), but most of the focus had been on the spatial patterns, environmental influences and interacting effects of CO₂ enhancement and N addition on carbon exchanges rates (Andersonteixeira et al., 2011; Falge et al., 2002; Wen et al., 2010; Yan et al., 2009; Yu et al., 2008). Meanwhile, previous studies on carbon fluxes in mangrove wetlands have mainly focused on the effects of meteorological events such as typhoons or hurricanes and tidal fluctuations on the ecosystem exchange of CO₂ or CH₄ and light use efficiency (Barr et al., 2012a, 2013, 2012b; Chen et al., 2014; Jha et al., 2014; Li et al., 2014).

In order to examine the differences in carbon fluxes and the underlying climate drivers between mangrove and terrestrial forest ecosystems, we compared the carbon flux traits and examined the different responses of carbon fluxes to climate parameters between two mangrove wetlands and two terrestrial forest ecosystems in subtropical China. Soil properties and tidal conditions were also examined to determine the possible mechanisms driving the different carbon flux characteristics between these two types of subtropical forest ecosystems. The specific objectives of this study were to 1) quantify the differences in the carbon fluxes values and dynamics between mangrove and terrestrial forest ecosystems, and 2) clarify the different mechanisms for regulating the responses of ecosystem CO₂ exchange to environmental factors in these forest ecosystems.

2. Materials and methods

2.1. Site description

The four sites are located between 20°N and 27°N in subtropical China and from the south to north they are Leizhou (LZ), Gaoqiao (GQ),

Dinghushan (DHS) and Qianyanzhou (QYZ) (Fig. 1). Among the four sites, the mangrove wetlands in LZ and GQ were composed of approximately 20-years-old artificial forests (*Sonneratia apetala*) and over 100-years-old natural mangrove forests, respectively. The terrestrial forests at DHS and QYZ were covered by over 400-years-old natural evergreen broad-leave forests (*Castanopsis chinensis*, *Schima asuperba* and *Cryptocarya chinensis*) and approximately 30-years-old manmade coniferous forest (*Pinus massoniana* Lamb, *Pinus elliottii* Engelm, *Cunninghamia lanceolata* Hook, *Schima crenata* Korthals and *Citrus L*), respectively. The average tree height at DHS was approximately 20 m, while the lowest average tree height at GQ site was approximately 4.5 m. The highest amount of soil organic carbon (SOC) was approximately 2.96% at GQ and the lowest was approximately 1.04% at QYZ (Table 1).

As the four sites are all in the subtropical zone of China, the air temperature (T_{air}), rainfall (precipitation) and photosynthetically active radiation (PAR) have significant seasonal dynamics. The annual mean T_{air} values at LZ, GQ, DHS and QYZ gradually decrease with the increasing latitude, which values are 24.5 °C, 23.2 °C, 20.4 °C and 18.2 °C, respectively (Fig. 2). The trends of annual mean precipitation are similar to those of T_{air} , and LZ experiences the most rainfall approximately 1619 mm per year, but there is less than 1000 mm of rainfall per year at QYZ. However, the annual mean PAR values of the four sites have no significant differences. The annual mean PAR values are approximately 260 $\mu\text{mol photons m}^{-2} \text{s}^{-1}$ at all sites, except DHS, where PAR is the lowest (233 $\mu\text{mol photons m}^{-2} \text{s}^{-1}$) probably due to the foggy days in this region during the wet season (Yu et al., 2008).

2.2. Carbon flux measurements and data processing

The carbon flux and microclimate data of the terrestrial forest ecosystems were measured from January 1, 2003 to December 31, 2005, and these data were provided by the ChinaFlux network. More details of the EC system structures at DHS and QYZ can be found in previous papers (Yu et al., 2008). According to the heights of plants in

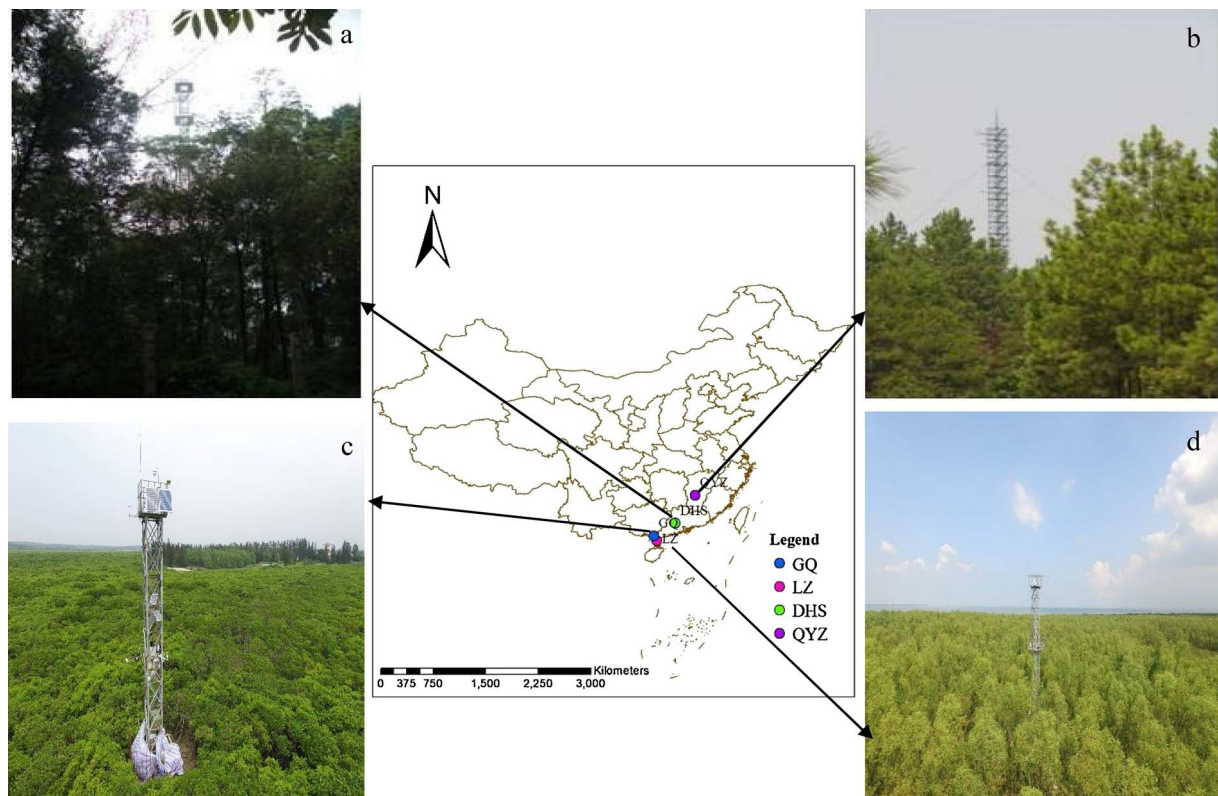


Fig. 1. Locations and vegetation pictures of four forest ecosystems with Eddy flux towers (a: Dinghushan (DHS), b: Qianyanzhou (QYZ), c: Gaoqiao (GQ) and d: Leizhou (LZ)).

Table 1

Information on the plants and soils at the four sites (GQ: Gaoqiao; LZ: Leizhou; DHS: Dinghushan; QYZ: Qianyanzhou). SOC and STN stand for the concentration of soil organic carbon and soil nitrogen, respectively.

Ecosystem	Sites	Plant				Soil		
		Age year	Height m	Type	Species	SOC %	STN %	Type
Mangrove	GQ	> 100	4.5	Natural	<i>Bruguiera gymnorrhiza</i> , <i>Aegiceras corniculatum</i> , <i>Kandelia obovate</i>	2.96	0.17	Coastal silty
	LZ	> 20	12	Manmade	<i>Sonneratia apetala</i>	1.27	0.13	Coastal silty
Terrestrial	DHS	> 100	20	Natural	<i>Castanopsis chinensis</i> , <i>Schin asuperba</i> , <i>Pinus massoniana</i>	2.61	0.24	Red soil
	QYZ	> 30	12	Manmade	<i>Pinus massoniana</i> Lamb, <i>Pinus elliottii</i> Engelm, <i>Cunninghamia lanceolata</i> Hook,	1.04	0.1	Lateritic red soil yellow soil

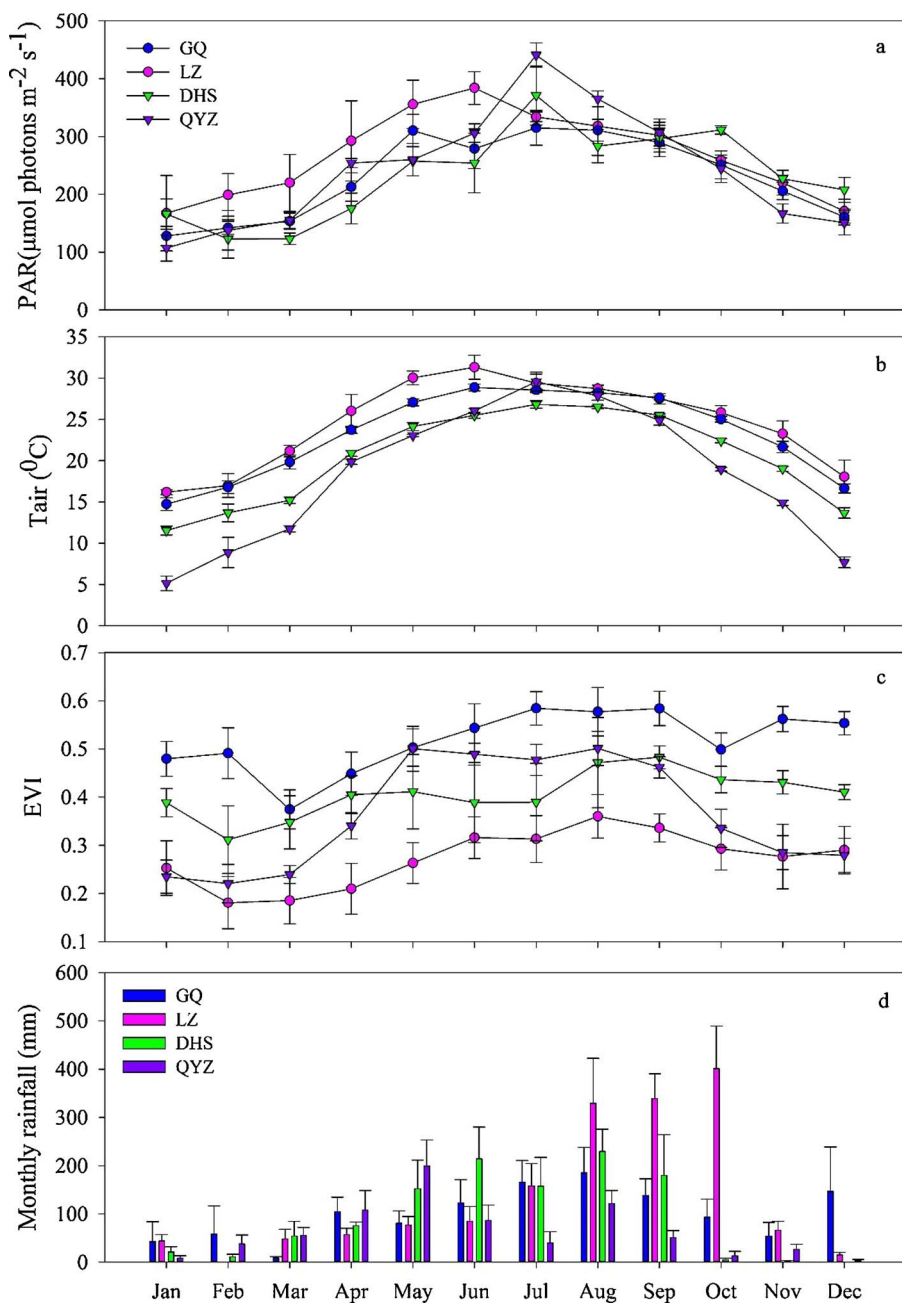


Fig. 2. Monthly variations in incident photosynthetically active radiation (PAR) (a), air temperature (T_{air}) (b), enhanced vegetation index (EVI) (c) and monthly cumulative rainfall (mm) (d). The abbreviations for the sites are the same as in Fig. 1.

the mangrove wetlands, the EC systems were mounted at 7 m and 18 m above the ground at GQ and LZ, respectively. Each EC systems for the two mangrove wetlands consisted of a three-dimensional sonic anemometer (CSAT3; Campbell Scientific, Inc., USA) and an open-path infrared CO₂ and H₂O gas analyzer (LI-7500; Li-Cor, Inc., USA). The

fluxes data were recorded by high-frequency measurement at 10 Hz, and logged at 30 min intervals using a data logger (CR1000; Campbell Scientific, Inc., USA). The microclimate parameters included air temperature, relative humidity (HMP45AC; Vaisala, Inc., Finland), radiation (pyranometer sensor: LI-200SZ; Li-Cor, Inc.; quantum sensor: LI-

190SZ; Li-Cor, Inc.; four component net-radiation sensor: NR01; Hukseflux Thermal Sensors, Inc., USA), wind speed (010C; Met One Instruments, Inc., USA), wind direction (020C; Met One Instruments, Inc., USA), soil temperatures (109; Campbell Scientific, Inc., USA) and rainfall (TE525MM; Texas Electronics, Inc., USA).

The data processing consisted of 4 steps: (1) flux calculation and correction: that was completed using Eddypro5.1, which is a software for CO₂, latent heat, sensible heat and H₂O flux calculations. There were several data problems to address in this step, such as axis rotation, ultrasonic correction, and frequency response correction (high and low frequency filtering). (2) Data quality control: we defined the valid flux regions using the footprints and the reasonable friction velocity (u_*) values to reduce the effect of insufficient turbulence. Moreover, the abnormal flux values were controlled by the standard deviation method, and a value was considered abnormal when it was 1.96 times larger than the standard deviation of 5 continuous values including itself (Eq. (1)). The ratios of missing carbon flux data of each site can be found in supplementary Table 1.

$$G_i = \frac{|NEE_i - \overline{NEE_n}|}{S_n} \quad (1)$$

where NEE_i is the NEE value of number i , while NEE_n and S_n stand for the average and standard error of 2 continuous values around NEE_i , respectively. The storage flux under the forest canopy was not estimated, because Baldocchi et al. (2000) considered that the long-term sum of the storage flux was zero (Baldocchi et al., 2000). (3) Gap-filling: the purpose of the EC method is to collect the $360d \times 24h$ fluxes data, but missing data often occurs during the field measurements. This study adapted the improved marginal distribution sampling (MDS) method (Reichstein et al., 2005) to fill the missing fluxes. (4) Flux partition: NEE was directly obtained, but estimating and analyzing the carbon balance in the ecosystem was required to partition the NEE data into gross ecosystem production (GEP) and ecosystem respiration (Re). In this study, the Re estimation was performed by dynamic fitting the short period data parameter, and this method was based on Reichstein's study on nighttime data (Reichstein et al., 2005). The Lloyd-Taylor model was used to represent the dependence of Re on temperature:

$$Re = Re_{ref} \times e^{E_0 \times \left(\frac{1}{T_{ref} - T_0} - \frac{1}{T - T_0} \right)} \quad (2)$$

where Re_{ref} is the respiration ratio at 20 °C (T_{air}), T_0 is a constant of -46.02 , and E_0 is a temperature sensitive parameter. The GEP is equal to the sum of $-NEE$ and Re . More information about the gap-filling and partition processing methods can be found in Liu (2015) and the data and method code are on website: <http://166.111.7.71/cproject/>

$$GEP = Re - NEE \quad (3)$$

2.3. Canopy dynamics and soil characteristics

Enhanced vegetation index (EVI) values reflect the vegetation signals on the ground and are sensitive to the plants canopy even in regions with the high biomass (Huete et al., 2002). This study adopted the EVI production of MOD13A1 from MODIS (<http://modis.gsfc.nasa.gov/>). The EVI values of the four sites are all in grid h28v06, and the data have a 16-day temporal resolution and 250 m spatial resolution. The ranges of EVI values are from 0 to 1 and high EVI values indicate broom canopy. As clouds might influence the EVI values, we selected the highest EVI values to represent the canopy condition of each month.

The soils under the mangrove forest stands around the EC towers at GQ and LZ were sampled. The depth of the soil cores was approximately 1 m and each soil core was divided into different layers including 0–10 cm, 10–20 cm, 20–40 cm, 40–60 cm, 60–80 cm and 80–100 cm. All soil cores were freeze-dried and grounded using a porcelain mortar and pestle, and the large particles and shoots or roots were removed by passing the samples through a 0.5 mm sieve. To eliminate total

inorganic carbon, the sieved soils were treated by the sulfuric acid-potassium dichromate oxidation method. The SOC and soil total nitrogen (STN) concentration were measured by a vario MACRO CUBE elemental analyzer (Elementar Analysensysteme GmbH, Germany). The carbon isotope ($\delta^{13}C$) of organic materials were determined by an isotope ratio mass spectrometer (Finnigan Delta V Advantage, Thermo Fisher Scientific, Inc.) in a joint stable isotope laboratory of Shenzhen City Huake Prevision Testing Technology, Inc. and Graduate School at Shenzhen, Tsinghua University. The $\delta^{13}C$ values express the isotope ratios of each soil layer:

$$\delta^{13}C = \left(\frac{R_{sample}}{R_{standard}} - 1 \right) \times 1000 \quad (4)$$

where $R_{sample} = (^{13}C/^{12}C)$ is the molar ratio of the heavy to light isotope of the soil and $R_{standard} = (^{13}C/^{12}C)$ is the ratio of Pee Dee Belemnite (PDB) standard (Cheng et al., 2006). The systematic error for the $\delta^{13}C$ measurement was less than 0.1‰ based on repeated measurements of an internal working standard, Protein (Elemental Microanalyses, Inc., China). In addition, we compiled the soil characteristics of terrestrial forests from two previous studies (Wang et al., 2011; Xiong et al., 2016).

2.4. Statistical analyses

To simulate the relationships between carbon fluxes and climate parameters, the Landsberg model (Chen et al., 2002) was used to express the dependence of NEE on PAR (Eq. (5)). As a result of the fitted relationships P_{max} (the maximum rate of photosynthesis) and P_{com} (the light compensation point, when $NEE=0$) were obtained for all four sites.

$$NEE = P_{max} \times (1 - e^{-\alpha(PAR - P_{com})}) \quad (5)$$

where α is the slope of the increases in P_{max} with PAR.

The Lloyd and Taylor model (Lloyd and Taylor, 1994) describes the response of Re to T_{air} (Eq. (2)). Based on the ecological meanings of E_0 in Eq. (2), it was related to temperature sensitivity (Q_{10}) (Eq. (6)):

$$Q_{10} = e^{10 \times E_0} \quad (6)$$

The tidal periods were recorded by a tide monitor (YSI E22-600LS) set a few meters away from our EC tower in the mangrove wetlands. The tide gauge equipment recorded the water level and salinity every 10 min. In this study, the tidal effects on the carbon fluxes of the mangroves were considered valid when the records showed water levels over 0.05m, which were considered spring tides, while those lower than 0.05 m were classified as neap tides. The differences in CO₂ fluxes among the four sites were tested using Tukey multiple comparisons in SPSS 19.0 (SPSS Inc., USA).

3. Results

3.1. Ecosystem carbon fluxes on annual and seasonal scales

All four study sites served as carbon sinks on an annual scale (Fig. 3a, b), and all points were above the 1:1 line of GEP vs. Re (Fig. 3c). However, the carbon sequestration capacities substantially varied among the four sites. The NEE values of the mangrove ecosystems were significantly lower than those of the nearby terrestrial forests. The lowest NEE value was $-1105.15 \pm 70.85 \text{ g C m}^{-2} \text{ y}^{-1}$ at LZ while the highest value was $-354.72 \pm 70.85 \text{ g C m}^{-2} \text{ y}^{-1}$ at QYZ. Meanwhile, the GEP values of the mangrove wetlands were significantly higher than those of terrestrial forests, and the values for GQ ($2101.77 \pm 164.89 \text{ g C m}^{-2} \text{ y}^{-1}$) and DHS ($1046.77 \pm 43.58 \text{ g C m}^{-2} \text{ y}^{-1}$) were the highest and lowest values, respectively. Moreover, the Re values in the mangrove wetlands were significantly lower than those in the terrestrial forests and the ratios of Re to GEP in the mangrove wetlands (LZ: 0.45 ± 0.02 , GQ: 0.63 ± 0.03) were

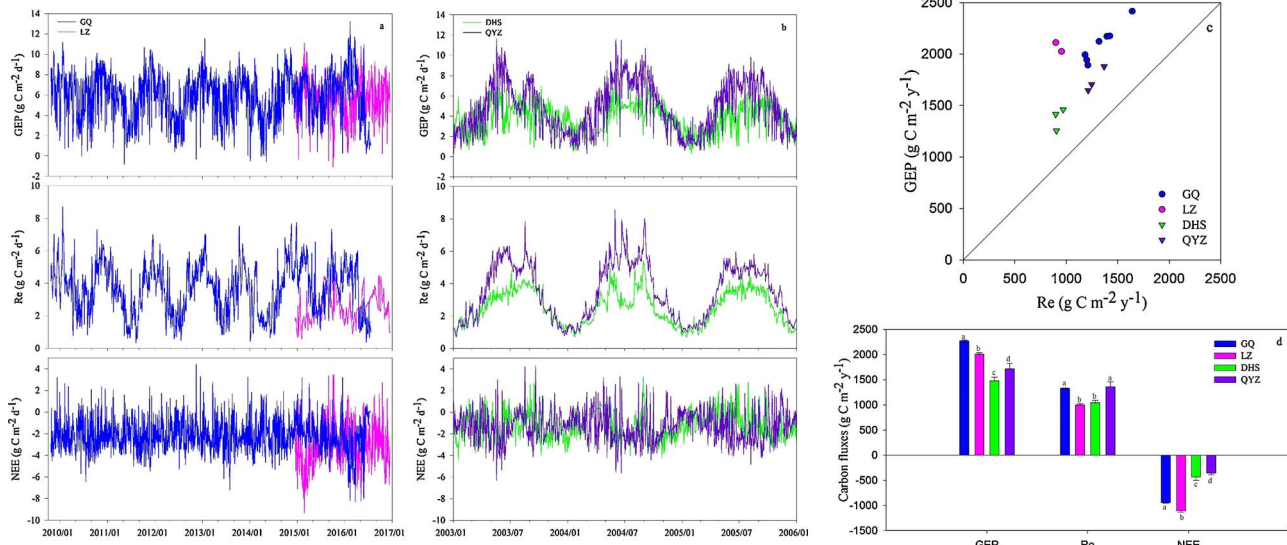


Fig. 3. The inter-annual dynamics of the daily values and the relationships of the annual mean values of gross ecosystem production (GEP), ecosystem respiration (Re) and net ecosystem exchange (NEE) among the four sites. (a: the carbon flux dynamics of the two mangrove wetlands of GQ and LZ; b: the carbon flux dynamics of the two terrestrial forests of DHS and QYZ; c: the GEP vs. Re among the four sites on a yearly scale; d: the analysis of the significant differences in the annual carbon fluxes among the four sites). The abbreviations for the sites are the same as in Fig. 1.

smaller than those for the terrestrial forests (DHS: 0.70 ± 0.04 , QYZ: 0.79 ± 0.01).

In the natural forests, the NEE values in the mangrove wetlands (GQ) were 117.23% lower than terrestrial forests (DHS). These NEE values were determined by 53.52% higher GEP and 27.02% higher Re values in mangrove wetlands compared to the terrestrial forests. However, for the plantations, the NEE value was 212.3% lower in the mangrove wetland (LZ site) than in the terrestrial forest (QYZ site); the GEP was 16.9% higher but the Re value was 26.6% lower in the mangrove wetlands (Fig. 3d).

3.2. Relationships between carbon fluxes and environmental parameters

The relations of NEE to PAR and Re to T_{air} were simulated by Eqs. (2) and (5), and the P_{max} , P_{com} , Re_{ref} and Q_{10} of each site were calculated (Table 2). The P_{max} value at LZ (approximately $3.97 \pm 0.52 \text{ g C } \mu\text{mol photons}^{-1}$) was significantly higher than that at the other three sites. The P_{com} value of both mangrove ecosystems were lower than those in the terrestrial forests (Table 2). Moreover, the light use efficiency (LUE) values of the mangrove wetlands were significantly higher than those of the terrestrial forests (Fig. 4a). Among the four sites, the LUE value of GQ ($0.026 \text{ g C } \mu\text{mol photons}^{-1}$) was significantly higher than the other three sites. The Re_{ref} was not significantly different between mangrove and terrestrial forest ecosystems; the highest value ($3.59 \pm 0.39 \text{ g C m}^{-2} \text{ s}^{-1}$) was found at QYZ and the lowest value ($2.17 \pm 0.22 \text{ g C m}^{-2} \text{ s}^{-1}$) was found at LZ (Table 2). However, the Q_{10} values of two mangrove wetlands were significantly higher than those of terrestrial forests with GQ being the largest (2.42 ± 0.11) and DHS the smallest (1.25 ± 0.11) (Fig. 4b).

Table 2

The average annual values of maximum photosynthetic rate (P_{max}), light compensation point (P_{com}), reference ecosystem respiration rate (Re_{ref}) and temperature sensitivity (Q_{10}) among the four sites. The abbreviations for the sites are the same as in Table 1.

Sites	P_{max} $\text{g C } \mu\text{mol photons}^{-1}$	P_{com} $\mu\text{mol photons}$	Re_{ref} $\text{g C m}^{-2} \text{ s}^{-1}$	Q_{10}
GQ	2.81 ± 0.11^a	43.40 ± 5.67^a	2.69 ± 0.49^a	2.42 ± 0.11^a
LZ	3.97 ± 0.52^b	51.10 ± 9.29^b	2.17 ± 0.22^b	1.31 ± 0.22^b
DHS	2.23 ± 0.31^c	67.55 ± 3.48^c	2.31 ± 0.18^b	1.25 ± 0.04^b
QYZ	2.69 ± 0.46^a	72.04 ± 12.15^c	3.59 ± 0.36^c	1.26 ± 0.04^b

Positive relations between EVI and GEP were observed in the terrestrial forests but those relations were not found in the mangrove wetlands (Fig. 5a, b). The relationships between Re and EVI indicated that Re was more sensitive to EVI in the manmade forests (LZ and QYZ) than in the natural forests (GQ and DHS) (Fig. 5c,d). The results of the soil data analysis showed a linear relationships between $\ln(\text{SOC})$ and $\delta^{13}\text{C}$. Slope values of -1.14 , -0.89 , -1.66 and -1.98 were found at GQ, LZ, DHS and QYZ, respectively, indicating higher slope values in the mangrove wetlands than in the terrestrial forests (Fig. 6).

3.3. Tidal conditions and relationships between ecosystem carbon fluxes and climate factors in mangrove wetlands

The P_{max} , P_{com} , Re_{ref} and Q_{10} values were significantly different between spring and neap tides in the mangrove ecosystems (Fig. 7, Table 3). Compared with no tide inundation period, the P_{max} increased by 43.2% at LZ during the spring tide, and this increase was larger than that at GQ (18.8%). Moreover, the P_{com} values decreased approximately 48.9% at GQ, but significantly increased by approximately 461.0% at LZ. Due to tidal inundation, the Re_{ref} values of both mangrove wetlands decreased approximately 5.8% and 10.9% at GQ and LZ, respectively. However, the Q_{10} values at GQ significantly increased and the increase ratio of GQ mangrove wetlands was 6.5 times larger than that of LZ mangrove wetlands during tidal flooding. In addition to the tidal flooding effects, the salinity also limited the LUE of mangrove plants. LUE had a significantly negative linear relationship with salinity at LZ. However, the LUE at GQ increased with salinity until salinity value reached 15 PSU and then decreased (Fig. 8).

4. Discussion

4.1. Differences in GEP, Re and NEE between mangrove wetlands and terrestrial forests

Our results showed that the lower NEE values of mangrove wetlands compared to those of terrestrial forests were determined by higher GEP but lower Re values (Fig. 3), which agreed well with a previous study in a subtropical mangrove ecosystem in the USA (Barr et al., 2010). However, NEE values reflect the CO_2 exchange between ecosystem and the atmosphere, and do not include horizontal carbon exchange

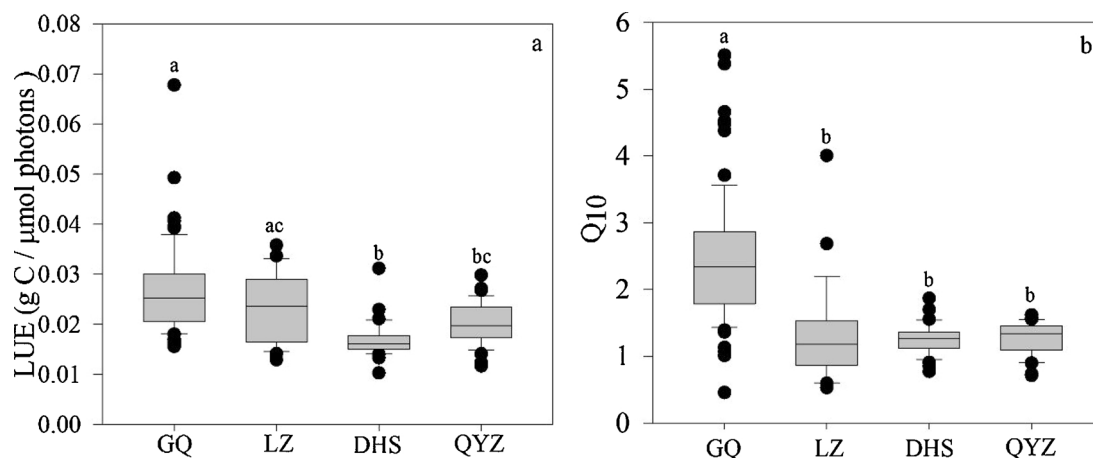


Fig. 4. The analysis of the significant differences in the monthly light use efficiency (LUE, a) and temperature sensitivity (Q_{10} , b) among the four sites. The abbreviations for the sites are the same as in Fig. 1.

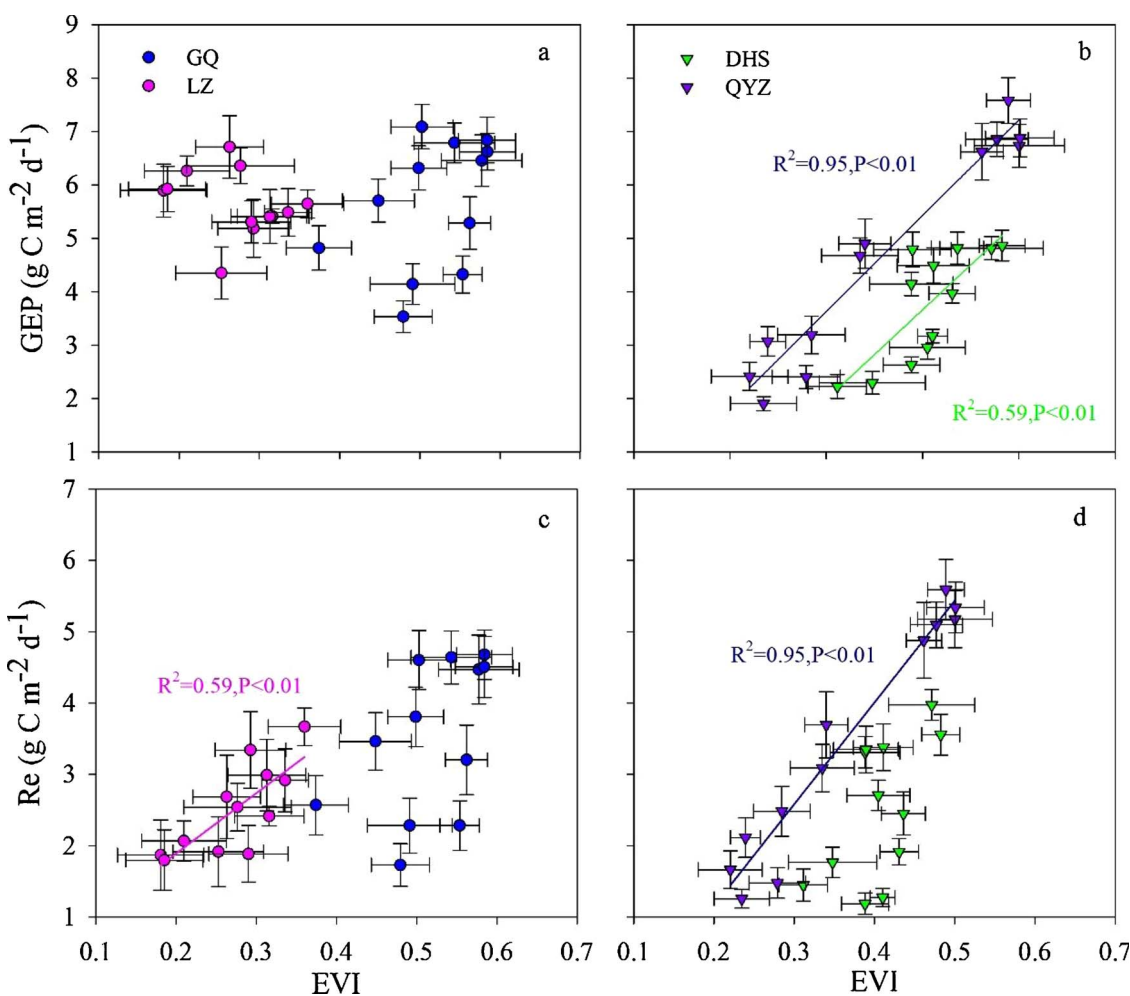


Fig. 5. Relationships between the monthly means of the daily GEP, Re and EVI values (a and c are the relationships between GEP, Re and EVI in the mangrove wetlands, b and d are the relationships between GEP, Re and EVI in the terrestrial forests). The abbreviations for the sites are the same as in Fig. 1.

between mangrove wetlands and tidal creeks. We obtained the NEE from eddy covariance measurements but the GEP and Re were simulated by a nighttime data-based method (Reichstein et al., 2005). The uncertainties of this model due to missing nighttime data were noted by some studies (Falge et al., 2001). However, other studies have concluded that there were no significant differences between this model and others on a yearly scale (Stoy et al., 2006).

Previous studies in the mangrove wetlands in Florida Everglades of USA showed that total amount of annual exported dissolve carbon, including dissolved inorganic carbon (DIC) and dissolved organic carbon (DOC) exported into coastal ocean was between 56 and 107.31 $\text{g C m}^{-2} \text{y}^{-1}$ (Romigh et al., 2006; Ho et al., 2017). According to these results, even when the dissolved carbon transported by tidal effects in mangrove wetlands is excluded, the annual carbon sinks of

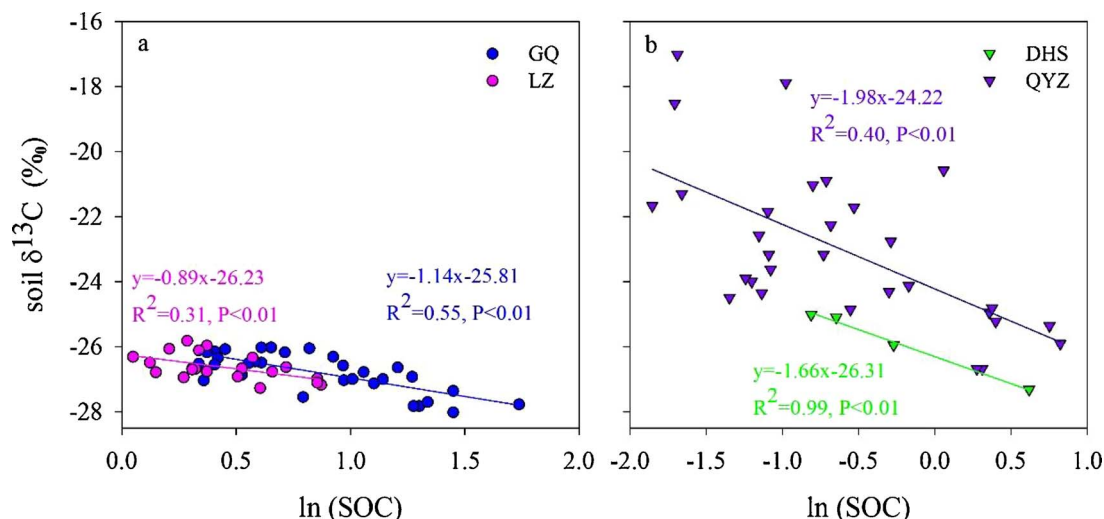


Fig. 6. Relationship between the logarithmic values of soil organic carbon (SOC) (ln(SOC)) and soil $\delta^{13}\text{C}$. The abbreviations for the sites are the same as in Fig. 1.

mangrove wetlands are still larger than those of the terrestrial forests in this study. Nevertheless, the conditions of the mangrove wetlands were different between our sites and the Florida Everglades sites. Thus, measuring the exchange in dissolved carbon via tidal creeks is necessary in future studies at our sites, because the variations in ecosystem carbon fluxes among different ecosystems are often controlled by meteorological parameters and the structures of forest ecosystems (Griffis et al., 2003; Law et al., 2002; Yu et al., 2008).

4.2. Strong influences of light use strategies on GEP in mangrove wetlands

In this study, we found that the GEP values in mangrove wetlands were significantly larger than those in terrestrial forests, which was likely caused by unique light use strategies of high P_{max} but low P_{com} values in mangrove ecosystems (Krauss et al., 2006). Previous studies demonstrated that there were strong positive relations between high production and thick canopy of forest ecosystems (Liu et al., 2015;

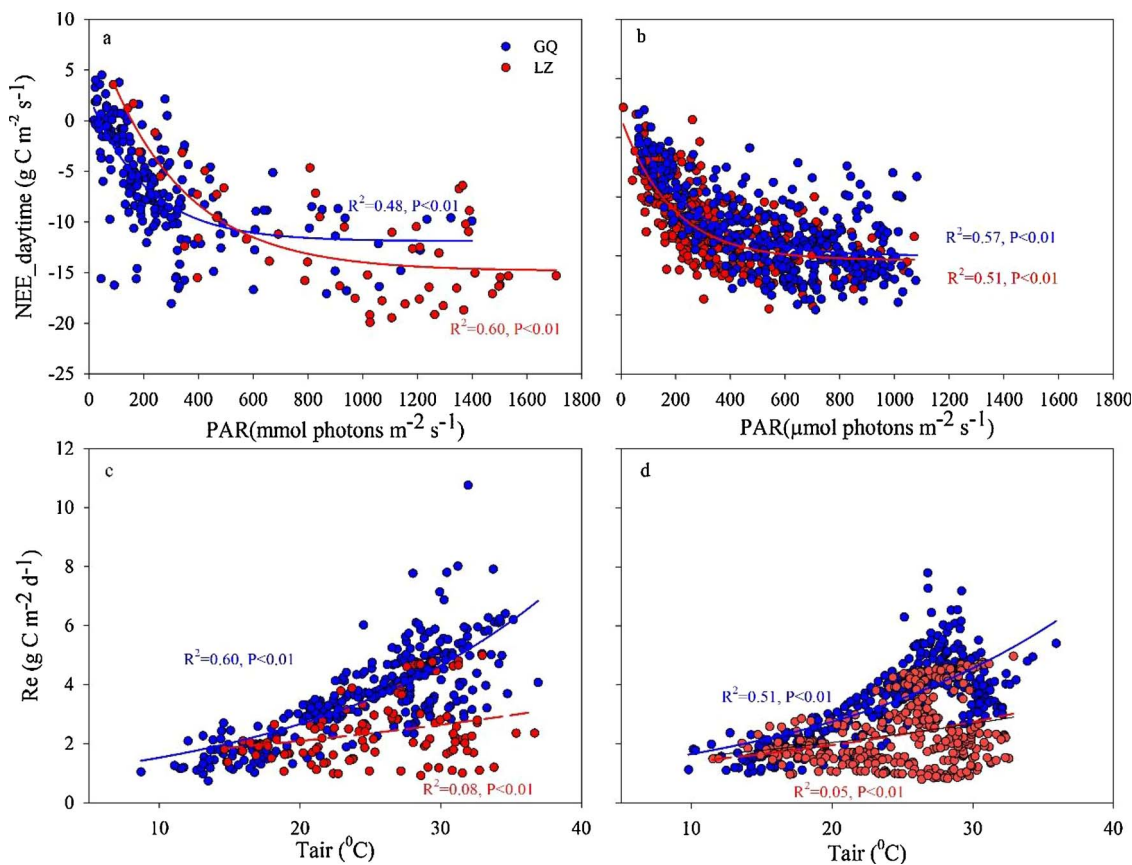


Fig. 7. Tidal effects on the relationships of $\text{NEE}_{\text{daytime}}$ to PAR and Re to T_{air} in mangrove wetlands in 2015 (a and c present the relationships during flooding, b and d present the relationships during non-flooding periods). The abbreviations for the sites are the same as in Fig. 1.

Table 3

The values of maximum photosynthetic rate (P_{max}), light compensation point (P_{com}), reference ecosystem respiration rate (Re_{ref}) and temperature sensitivity (Q_{10}) values under flooding and non-flooding periods in the mangrove wetlands (the P_{max} and P_{com} are the values during the daytime, and the Re_{ref} and Q_{10} are on a daily scale). The abbreviations for the sites are the same as in Table 1.

	Flooding		No flooding	
	GQ	LZ	GQ	LZ
P_{max} (g C $\mu\text{mol photons}^{-1}$)	11.89	14.84	10.01	10.36
P_{com} ($\mu\text{mol photons}$)	37.89	154.45	68.78	27.53
Re_{ref} (g C $\text{m}^{-2} \text{s}^{-1}$)	2.61	2.04	2.77	2.29
Q_{10}	2.93	1.41	1.62	1.26

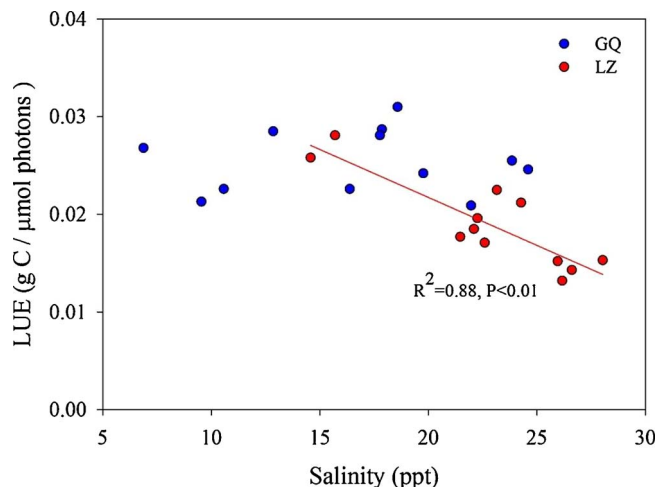


Fig. 8. Relationships between the monthly mean values of salinity and LUE in the mangrove wetlands in 2015. The abbreviations for the sites are the same as in Fig. 1.

Miller, 1972). However, the GEP values were significantly positively related to EVI in both terrestrial forests, but this relationship was not significant in either mangrove wetland. This result was probably because the EVI values were mismatched with the GEP values during the typhoon season (from May to October) (Chen et al., 2014). Furthermore, the climate conditions such as PAR and T_{air} were also the key controlling factors for the different GEP values among the mangrove wetlands and terrestrial forests (Yu et al., 2008). The lowest PAR values in natural forests at DHS were mainly caused by the fog during the wet season, which caused significantly lower GEP values at DHS than in the natural mangrove wetlands at GQ. Moreover, the lowest annual mean temperature in the manmade forest at QYZ limited the GEP values, which were significantly lower than those at LZ.

Under suitable climate conditions and strong light use strategies, the LUE values of mangrove wetlands were limited by salinity that caused photoinhibition on mangrove plants (Field et al., 1998), which indicated the GEP values of mangrove wetlands were controlled by the interactive effects of light and salinity. Previous studies at the leaf and plant levels showed similar results, and plants were found to gain more carbon at low salinities than at high salinities, because the stomatal limitations and high respiratory costs at high salinities restrict the responses of plants to light result in more sequestered carbon (Ball, 2002; Krauss and Allen, 2003; Lopez-Hoffman et al., 2007). Here, our results also showed that high salinity limited LUE of mangrove plants, but the relationships between salinity and LUE at GQ and LZ were different. The reason for this difference was due to the difference in suitable salinities for plants that were about 10 and 15 PSU at LZ and GQ site, respectively (Chen et al., 2000), which also explained the lower GEP values at LZ than those at GQ.

4.3. The anomalies of Re in mangrove wetlands

A previous study suggested that plants were the main source of Re in plantations, while soil respiration dominated Re in natural forests (Yu et al., 2004). Our results were consistent with this finding as annual mean Re in the mangrove plantation at LZ was significantly lower than that at QYZ even though the SOC concentration at LZ was a higher than that at QYZ. This difference might be caused by a thicker canopy, which resulting in a higher Re_{ref} at QYZ than at LZ. Meanwhile, the Re_{ref} values at GQ and DHS were similar, but the higher Q_{10} values at GQ caused the mean Re value to be significantly higher at GQ than at DHS. Moreover, the observations of higher SOC and T_{air} values but lower annual mean Re values in the mangrove wetlands than in the nearby terrestrial forests was surprising.

Previous studies established a linear relationship between soil $\delta^{13}\text{C}$ values and $\ln(\text{SOC})$ to explain C turnover time or SOC decomposition rates (Harden et al., 2002; Wang et al., 2011). The slopes of $\delta^{13}\text{C}$ to $\ln(\text{SOC})$ at both mangrove sites were larger than those of terrestrial forest ecosystems (Fig. 6), which indicated the lower SOC decomposition rates. Moreover, the $\delta^{13}\text{C}$ values were negatively related to SOC in terrestrial forests, which was also consistent with a previous study that found water stress resulted in more accumulating of SOC decomposition rates in terrestrial forests than in mangrove wetlands (Feng et al., 2017; Li et al., 2013). Thus this finding explains the lower Re values of the mangrove wetlands compared to those of terrestrial forests.

4.4. Tidal influences on the relationships of carbon fluxes to climate variables

Periodic tidal inundation is the unique disturbance in mangrove wetlands compared to terrestrial ecosystems, and changes the salinity and depth of soil water for the mangrove plants. Previous studies indicated the response of GEP to light was limited by salinity, while flooding limited soil Re in mangrove wetlands (Ball and Farquhar, 1984; Clough, 1984; Li et al., 2014; Sobrado, 1999). However, mangrove plants have evolved some adaptation strategies such as conservative water use, high P_{max} and low P_{com} (Cheeseman and Lovelock, 2004; Krauss et al., 2006). In the mangrove wetlands studied here, the P_{max} increased during spring tide, which was consistent with a previous study (Li et al., 2014). However, P_{com} decreased at GQ but increased at LZ mangrove wetlands (Fig. 7), which might be due to the weak resistances of mangrove vegetation to the salinity at LZ (Chen et al., 2000). Moreover, the Re anomalies in the mangrove wetlands might be influenced by the effects of flooding and salinity tides (Barr et al., 2010; Hwang and Chen, 2001). The Re_{ref} at both mangrove sites decreased when mangrove soils were submerged, but the Q_{10} values were significantly higher (Table 3), which could be a result of high CO_2 emission from tide water as the temperature increased (Maher et al., 2015). In total, the NEE values in GQ mangrove wetlands decreased during flooding, because both the GEP and Re values decreased and the ratios of the GEP decreased were larger than those of Re . However, the NEE values at LZ during flooding increased due to the higher GEP but lower Re values compared to without flooding times. These different results between the two mangrove wetlands were determined by the different flooding times, as the flooding mainly occurred between 10:00 am and 18:00 pm at LZ but was scattered at any time at GQ (Fig. 9). In addition, it is important to note that tidal effects increase the uncertainty of estimating ecosystem CO_2 exchange by EC measurements, because the tides export DIC from mangrove wetlands that would lower the Re (Barr et al., 2010).

5. Conclusions

By analyzing the carbon fluxes from four flux towers, this study examined the carbon sequestration potential between mangrove and terrestrial forest ecosystems. Lower NEE values indicated that carbon

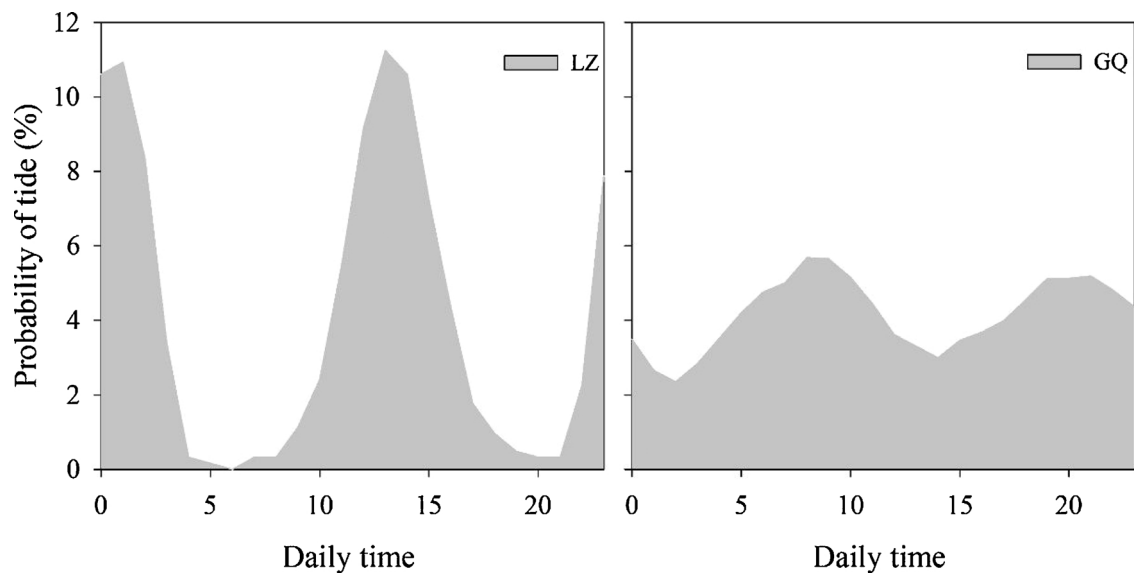


Fig. 9. The flooding probability of tides at Gaoqiao (GQ) and Leizhou (LZ). The tide at GQ cycles once a day (typical diurnal tide) whereas the tide at LZ twice a day (semi-diurnal tide).

sequestration potential of mangrove wetlands was stronger than that of terrestrial forests. Higher GEP values resulted from advantages of light use strategies and climate conditions, and lower Re values that were caused by lower Re_{ref} values resulted from lower SOC decomposition rates of mangrove wetlands compared to those of terrestrial forests. In addition, tidal effects changed the relationships between carbon flux and climate factors, such as increased the P_{max} and Q_{10} in mangrove wetlands during flooding and non-flooding periods. Altogether, our study provides a fundamental understandings of the differences in carbon sequestration capacities between subtropical mangrove wetlands and nearby terrestrial forests. The tidal regulations of mangrove ecosystem CO_2 fluxes should be investigated in more detail in future studies.

Acknowledgments

The lead author would like to express great gratitude to Guiri Yu at Institute of Geography and Natural Resources, Chinese Academy of Sciences for his suggestions and encouragement during the mangrove flux measurements and the preparation of this manuscript. We thank the staff at our two mangrove flux tower sites for maintaining the continuous flux measurements over many years, and Guoyi Zhou and Huimin Wang for providing the eddy flux data from the Dinghushan (DHS) and Qianyanzhou (QYZ) sites, respectively. We also thank many team members of our group especially Jian Zhou, Weixiu Gan, Liming Wang, Jiankun Bai and Genghong Wu for setting up the flux towers, collecting flux data or processing the flux data for the two mangrove sites. We acknowledge the financial support from The National Key Basic Research Program (973), Ministry of Science and Technology, China (2013CB956601), Shenzhen Basic Research Discipline Layout Project, Shenzhen Science and Technology Innovation Committee, China (JCYJ20150529164918736) and the Ocean Open Public Fund Project, State Oceanic Administration, China (201305021).

Appendix A. Supplementary data

Supplementary data associated with this article can be found, in the online version, at <http://dx.doi.org/10.1016/j.agrformet.2017.11.019>.

References

Andersonteixeira, K.J., et al., 2011. Differential responses of production and respiration to temperature and moisture drive the carbon balance across a climatic gradient in New

- Mexico. *Global Change Biol.* 17 (1), 410–424.
- Artigas, F., et al., 2015. Long term carbon storage potential and CO_2 sink strength of a restored salt marsh in New Jersey. *Agric. Forest Meteorol.* 200, 313–321.
- Baldocchi, D., et al., 2000. On measuring net ecosystem carbon exchange over tall vegetation on complex terrain. *Bound-Lay Meteorol.* 96 (1–2), 257–291.
- Baldocchi, D., 2008. Breathing of the terrestrial biosphere: lessons learned from a global network of carbon dioxide flux measurement systems. *Aust. J. Bot.* 56 (1), 1–26.
- Ball, M.C., Farquhar, G.D., 1984. Photosynthetic and Stomatal Responses of 2 Mangrove Species, *Aegiceras-Corniculatum* and *Avicennia-Marina*, to Long-Term Salinity and Humidity Conditions. *Plant Physiol.* 74 (1), 1–6.
- Ball, M.C., 2002. Interactive effects of salinity and irradiance on growth: implications for mangrove forest structure along salinity gradients. *Trees-Struct. Funct.* 16 (2–3), 126–139.
- Barr, J.G., et al., 2010. Controls on mangrove forest-atmosphere carbon dioxide exchanges in western Everglades National Park. *J. Geophys. Res.-Biogeo.* 115.
- Barr, A.G., et al., 2012a. Energy balance closure at the BERMS flux towers in relation to the water balance of the White Gull Creek watershed 1999–2009. *Agric. Forest Meteorol.* 153, 3–13.
- Barr, J.G., et al., 2012b. Hurricane disturbance and recovery of energy balance, CO_2 fluxes and canopy structure in a mangrove forest of the Florida Everglades. *Agric. Forest Meteorol.* 153, 54–66.
- Barr, J.G., et al., 2013. Modeling light use efficiency in a subtropical mangrove forest equipped with CO_2 eddy covariance. *Biogeosciences* 10 (3), 2145–2158.
- Bouillon, S., et al., 2008. Mangrove production and carbon sinks: a revision of global budget estimates. *Global Biogeochem. Cycl.* 22, GB2013. <http://dx.doi.org/10.1029/2007GB003052>.
- Bracho, R., et al., 2012. Controls on carbon dynamics by ecosystem structure and climate for southeastern US slash pine plantations. *Ecol. Monogr.* 82 (1), 101–128.
- Brummer, C., et al., 2012. How climate and vegetation type influence evapotranspiration and water use efficiency in Canadian forest, peatland and grassland ecosystems. *Agric. Forest Meteorol.* 153, 14–30.
- Cheeseman, J.M., Lovelock, C.E., 2004. Photosynthetic characteristics of dwarf and fringe *Rhizophora mangle* L. in a Belizean mangrove. *Plant Cell Environ.* 27 (6), 769–780.
- Chen, Changping, et al., 2000. Influences of salinity on the growth and some ecophysiological characteristics of mangrove species, *sonneratia apetala* seedlings. *Chin. Bull. Bot.* 17 (5), 457–461.
- Chen, J., et al., 2002. Biophysical controls of carbon flows in three successional Douglas-fir stands based on eddy-covariance measurements. *Tree Physiol.* 22 (2–3), 169–177.
- Cheng, X.L., et al., 2006. Short-term C-4 plant *Spartina alterniflora* invasions change the soil carbon in C-3 plant-dominated tidal wetlands on a growing estuarine Island. *Soil Biol. Biochem.* 38 (12), 3380–3386.
- Chen, H., et al., 2014. Typhoons exert significant but differential impacts on net ecosystem carbon exchange of subtropical mangrove forests in China. *Biogeosciences* 11 (19), 5323–5333.
- Clough, B.F., 1984. Growth and salt balance of the mangroves *avicennia-marina* (Forsk) vierh and *rhizophora-stylosa* griff in relation to salinity. *Aust. J. Plant Physiol.* 11 (5), 419–430.
- Coursolle, C., et al., 2006. Late-summer carbon fluxes from Canadian forests and peatlands along an east-west continental transect. *Can. J. For. Res.* 36 (3), 783–800.
- Donato, D.C., et al., 2011. Mangroves among the most carbon-rich forests in the tropics. *Nat. Geosci.* 4 (5), 293–297.
- Falge, E., et al., 2001. Gap filling strategies for defensible annual sums of net ecosystem exchange. *Agric. Forest Meteorol.* 107 (1), 43–69.
- Falge, E., et al., 2002. Seasonality of ecosystem respiration and gross primary production as derived from FLUXNET measurements. *Agric. Forest Meteorol.* 113 (1–4), 53–74.
- Feng, W., et al., 2017. Enhanced decomposition of stable soil organic carbon and

- microbial catabolic potentials by long-term field warming. *Global Change Biol.* 2017, 1–12.
- Field, C.B., et al., 1998. Mangrove biodiversity and ecosystem function. *Global Ecol. Biogeogr.* 7 (1), 3–14.
- Griffis, T.J., et al., 2003. Ecophysiological controls on the carbon balances of three southern boreal forests. *Agric. Forest Meteorol.* 117 (1–2), 53–71.
- Harden, J.W., et al., 2002. Cycling of beryllium and carbon through hillslope soils in Iowa. *Biogeochemistry* 60 (3), 317–335.
- Ho, D.T., et al., 2017. Dissolved carbon biogeochemistry and export in mangrove-dominated rivers of the Florida Everglades. *Biogeosciences* 14 (9), 2543–2559.
- Huete, A., et al., 2002. Overview of the radiometric and biophysical performance of the MODIS vegetation indices. *Remote Sens. Environ.* 83 (1–2), 195–213.
- Hwang, Y., Chen, S.-C., 2001. Effects of ammonium, phosphate, and salinity on growth, gas exchange characteristics, and ionic contents of seedlings of mangrove *Kandelia candel* (L.) Druce. *Bot. Bull. Acad. Sin.* 42 (2), 131–139.
- Jha, C.S., et al., 2014. Eddy covariance based methane flux in Sundarbans mangroves, India. *J. Earth Syst. Sci.* 123 (5), 1089–1096.
- Jung, M., et al., 2011. Global patterns of land-atmosphere fluxes of carbon dioxide, latent heat, and sensible heat derived from eddy covariance, satellite, and meteorological observations. *J. Geophys. Res.-Biogeophys.* 116.
- Krauss, K.W., Allen, J.A., 2003. Influences of salinity and shade on seedling photosynthesis and growth of two mangrove species, *Rhizophora mangle* and *Bruguiera sexangula*, introduced to Hawaii. *Aquat. Bot.* 77 (4), 311–324.
- Krauss, K.W., et al., 2006. Leaf gas exchange characteristics of three neotropical mangrove species in response to varying hydroperiod. *Tree Physiol.* 26 (7), 959–968.
- Law, B.E., et al., 2002. Environmental controls over carbon dioxide and water vapor exchange of terrestrial vegetation. *Agric. Forest Meteorol.* 113 (1–4), 97–120.
- Li, D.J., et al., 2013. Differential responses of soil organic carbon fractions to warming: results from an analysis with data assimilation. *Soil Biol. Biochem.* 67, 24–30.
- Li, Q., et al., 2014. Differential responses of net ecosystem exchange of carbon dioxide to light and temperature between spring and neap tides in subtropical mangrove forests. *Sci. World J.*
- Liu, M., et al., 2015. The effects of constraining variables on parameter optimization in carbon and water flux modeling over different forest ecosystems. *Ecol. Modell.* 303, 30–41.
- Liu, F., 2015. Comparison Research of Carbon Flux and Energy Exchange in Subtropical Mangrove Ecosystem [D]. Tsinghua University.
- Lloyd, J., Taylor, J.A., 1994. On the temperature-dependence of soil respiration. *Funct. Ecol.* 8 (3), 315–323.
- Lopez-Hoffman, et al., 2007. Salinity and light interactively affect neotropical mangrove seedlings at the leaf and whole plant levels. *Oecologia* 150 (4), 545–556.
- Lu, X.H., et al., 2014. Comparing simulated carbon budget of a lei bamboo forest with flux tower data. *Terr. Atmos. Ocean Sci.* 25 (3), 359–368.
- Lu, W., et al., 2017. Contrasting ecosystem CO₂ fluxes of inland and coastal wetlands: a meta-analysis of eddy covariance data. *Global Change Biol.* 23 (3), 1180–1198.
- Lund, M., et al., 2010. Variability in exchange of CO₂ across 12 northern peatland and tundra sites. *Global Change Biol.* 16 (9), 2436–2448.
- Maher, D.T., et al., 2015. Methane and carbon dioxide dynamics in a subtropical estuary over a diel cycle: insights from automated in situ radioactive and stable isotope measurements. *Mar. Chem.* 168, 69–79.
- McLeod, E., et al., 2011. A blueprint for blue carbon: toward an improved understanding of the role of vegetated coastal habitats in sequestering CO₂. *Front. Ecol. Environ.* 9 (10), 552–560.
- Miller, P.C., 1972. Bioclimate, leaf temperature, and primary production in red mangrove canopies in South Florida. *Ecology* 53 (1) 22–8.
- Moffat, A.M., et al., 2007. Comprehensive comparison of gap-filling techniques for eddy covariance net carbon fluxes. *Agric. Forest Meteorol.* 147 (3–4), 209–232.
- Piao, S.L., et al., 2009. The carbon balance of terrestrial ecosystems in China. *Nature* 458 (7241) 1009–U82.
- Polsenaere, P., et al., 2012. Spatial and temporal CO₂ exchanges measured by Eddy Covariance over a temperate intertidal flat and their relationships to net ecosystem production. *Biogeosciences* 9 (1), 249–268.
- Reichstein, M., et al., 2005. On the separation of net ecosystem exchange into assimilation and ecosystem respiration: review and improved algorithm. *Global Change Biol.* 11 (9), 1424–1439.
- Romigh, M.M., Davis, S.E., Rivera-Monroy, V.H., Twilley, R.R., 2006. Flux of organic carbon in a riverine mangrove wetland in the Florida Coastal Everglades. *Hydrobiologia* 569, 505–516.
- Sobrado, M.A., 1999. Leaf photosynthesis of the mangrove *Avicennia germinans* as affected by NaCl. *Photosynthetica* 36 (4), 547–555.
- Stoy, P.C., et al., 2006. An evaluation of models for partitioning eddy covariance-measured net ecosystem exchange into photosynthesis and respiration. *Agric. Forest Meteorol.* 141 (1), 2–18.
- Tan, Z.H., et al., 2011. An old-growth subtropical Asian evergreen forest as a large carbon sink. *Atmos. Environ.* 45 (8), 1548–1554.
- Wang, S.Q., et al., 2011. Effects of afforestation on soil carbon turnover in China's subtropical region. *J. Geogr. Sci.* 21 (1), 118–134.
- Wen, X.F., et al., 2010. Ecosystem carbon exchanges of a subtropical evergreen coniferous plantation subjected to seasonal drought, 2003–2007. *Biogeosciences* 7 (1), 357–369.
- Wilson, S.R., et al., 2007. Changes in tropospheric composition and air quality due to stratospheric ozone depletion and climate change. *Photochem. Photobiol. Sci.* 6 (3), 301–310.
- Xiao, J.F., et al., 2011a. Upscaling carbon fluxes from towers to the regional scale: influence of parameter variability and land cover representation on regional flux estimates. *J. Geophys. Res.-Biogeophys.* 116.
- Xiao, J.F., et al., 2011b. Assessing net ecosystem carbon exchange of U. S. terrestrial ecosystems by integrating eddy covariance flux measurements and satellite observations. *Agric. Forest Meteorol.* 151 (1), 60–69.
- Xiong, X., et al., 2016. 13C and 15N isotopic signatures of plant-soil continuum along a successional gradient in Dinghushan Biosphere Reserve. *Chin. J. Plant Ecol.* 40 (6), 533–542.
- Yan, H.M., et al., 2009. Modeling gross primary productivity for winter wheat-maize double cropping System using MODIS time series and CO₂ eddy flux tower data. *Agric. Ecosyst. Environ.* 129 (4), 391–400.
- Yi, C.X., et al., 2010. Climate control of terrestrial carbon exchange across biomes and continents. *Environ. Res. Lett.* 5 (3), 54–63.
- Yu, Guirui, et al., 2004. Seasonal patterns and environmental response characteristics of respiration in typical forest ecosystems in subtropical and temperate regions of China. *Sci. China Series D* 84–94.
- Yu, G.R., et al., 2008. Environmental controls over carbon exchange of three forest ecosystems in eastern China. *Global Change Biol.* 14 (11), 2555–2571.
- Yu, G., et al., 2011. Research on carbon budget and carbon cycle of terrestrial ecosystems in regional scale: a review. *Acta Ecol. Sin.* 31 (19), 5449–5459.
- Yu, G.R., et al., 2013. Spatial patterns and climate drivers of carbon fluxes in terrestrial ecosystems of China. *Global Change Biol.* 19 (3), 798–810.